03 Apr 1995, 4:00 pm - 5:00 pm

Dynamic Soil Pressures on Vertical Walls

Anestis S. Veletsos
Rice University, Houston, TX

Adel H. Younan
Rice University, Houston, TX

Proceedings: Third International Conference on Recent Advances in Geotechnical Earthquake Engineering and Soil Dynamics
April 2-7, 1995; Volume III, St. Louis, Missouri

STATE OF THE ART (SOA15)
Dynamic Soil Pressures on Vertical Walls

Anestis S. Veletsos
Rice University
Houston, TX, USA

Adel H. Younan
Rice University
Houston, TX, USA

SYNOPSIS: A summary is presented of recently contributed simple approximate solutions for the dynamic pressures and the associated forces induced by ground shaking on rigid vertical walls. The walls are presumed to be either straight or circular in plan and to retain a uniform viscoelastic soil stratum of constant thickness and infinite extent in the horizontal direction. Both the walls and the stratum are considered to be supported on a non-deformable base undergoing a space-invariant, uniform horizontal motion. The effects of both harmonic and earthquake-induced excitations are examined, and comprehensive numerical data are presented which elucidate the underlying response mechanisms and the effects and relative importance of the various parameters involved. A brief review is then included of available simple, approximate schemes for modeling the systems examined. Finally, the sources and magnitudes of the errors that may result from the use of these models are identified, and modifications are proposed with which the responses of the systems may be defined correctly. In the proposed modifications, the soil stratum is modeled by a series of elastically supported semiinfinite layers with distributed mass. The concepts involved are introduced for the straight wall and are then applied to the embedded cylindrical system.

INTRODUCTION

This paper examines the dynamic soil pressures and associated forces induced by ground shaking on straight and cylindrical vertical walls. The evaluation of these effects is fundamental to the seismic analysis and design of earth retaining systems and of embedded and underground structures.

The problem considered has been the subject of numerous studies over the years, and a number of methods and computer programs of varying degrees of accuracy, efficiency and sophistication have been developed for its solution. Valuable accounts of the previous contributions on straight walls have been provided in state-of-the-art reports by Nazarian and Hadjian (1979), Prakash (1981) and Whitman (1991), and a broad overview of the contributions on embedded cylindrical structures may be gained from the papers in the proceedings of the workshop on the analysis and interpretation of the seismic response data obtained from the nuclear power plant test model in Lotung, Taiwan (1989) and from a subsequent report on the same topic by Hadjian et al (1991).

The methods of analysis used for retaining walls may conveniently be classified into three groups: (1) those in which the relative motions of the wall and the backfill material are sufficiently large to induce a limit or failure state in the soil; (2) those in which the ground motion is of sufficiently low intensity so that the retained material may be considered to respond within the linearly elastic range of deformations; and (3) the intermediate case, in which the true non-linear, hysteretic properties of the soil are accounted for explicitly. Representative of the first approach is the well-known Mononobe-Okabe method (1929, 1924) and its various variants (Seed and Whitman 1970, Sherif et al 1982, 1984), and representative of the third approach is a recent contribution by Siller et al (1991) dealing with the responses of gravity and anchored walls. The following discussion is in the vein of the second approach in that the soil is modeled as an elastic or viscoelastic material.

Despite the value of the information contributed so far, however, the dynamic response of these soil-wall systems is still not well understood. There is, in particular, a lack not only of adequate numerical data that elucidate the underlying response mechanisms, but also of methods of analysis that are both rational and simple and may, therefore, be used reliably and cost-effectively in design.

The objective of the studies summarized here has been twofold: (1) to use existing or suitable improvements of existing methods to study critically the responses of classes of systems for which relatively simple analytical solutions are

possible; and (2) to assess the reliability of the simpler available methods which are particularly useful for preliminary design purposes and, where necessary, to propose appropriate improvements. Both straight and cylindrical walls are examined, with the soil medium presumed to respond within the linearly elastic range of deformations. Simple, approximate expressions for the critical responses of the systems are formulated, and comprehensive numerical data are presented which elucidate the underlying response mechanisms and the effects and relative importances of the numerous parameters involved.

The studies summarized here were carried out at Rice University (Veletsos and Younan 1994a, 1994b, 1994c, 1995) and were motivated by the need for improved understanding of the response to earthquakes of underground cylindrical tanks storing nuclear wastes, and for rational but simple methods of analysis and design for such systems. The analysis of these systems is highly complex, requiring consideration of the interaction effects not only between the oscillating liquid and the tank, but also between the tank and the concrete vault within which the tank may be encased, and between the tank-vault system and surrounding soil.

SYSTEM CONSIDERED

The system examined is shown in Fig. 1. It consists of a rigid circular cylinder of radius R that is embedded in a soil layer of constant thickness H and infinite extent in the horizontal direction. Idealized as a homogeneous viscoelastic material with frequency-independent properties, the soil layer is free at the upper surface and bonded along its lower boundary to a non-deformable, rigid base. The interface between the cylinder and surrounding soil may be either rough or smooth, as explained in greater detail in later sections. Both the cylinder and the base of the layer are assumed to undergo a space-invariant, uniform horizontal motion, the acceleration of which at any time t is $\ddot{x}_g(t)$. Points in the medium are defined by the cylindrical coordinate system, r, θ, z, the origin of which is taken at the center of the base of the cylinder, with θ positive in the counter-clockwise direction and $\theta = 0$ coinciding with the positive direction of the ground motion. For the limiting case of $R \to \infty$ or $H/R \to 0$, the cylindrical system considered reduces to the one shown in Fig. 2, in which a straight wall retains a semiinfinite, uniform viscoelastic stratum.

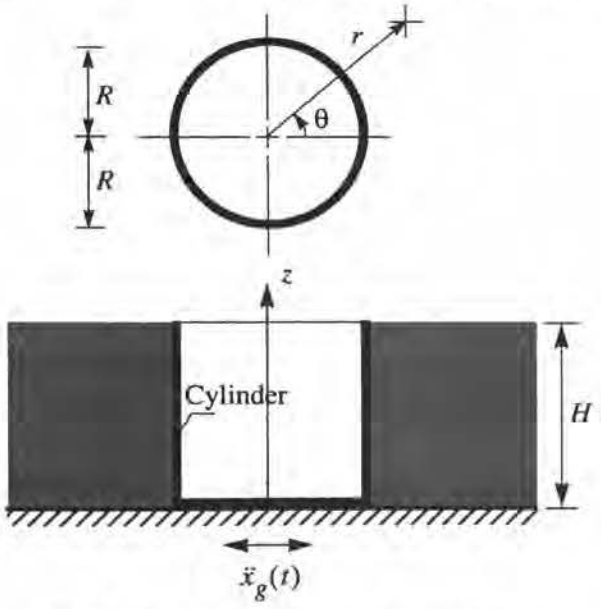

Fig. 1 Cylindrical System Considered

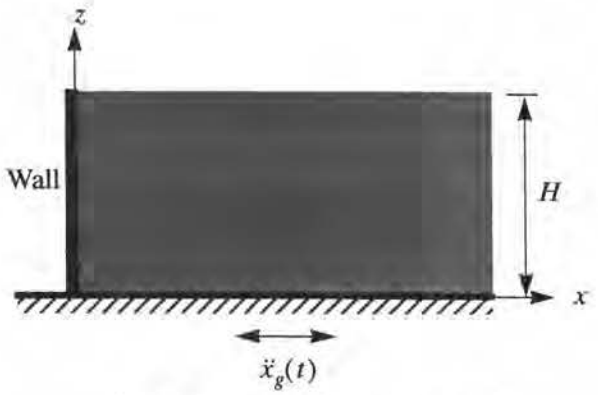

Fig. 2 System with straight wall

The properties of the stratum are defined by its mass density ρ, shear modulus G, Poisson's ratio ν, and the material damping factor δ, which is considered to be frequency-independent and the same for both shearing and axial deformations. The latter factor is the same as the $tan\delta$ factor used by the senior author and his associates in studies of foundation dynamics and soil-structure interaction (e.g., Veletsos and Verbic 1973, Veletsos and Dotson 1988), and twice as large as the fraction of critical damping, β, used by other authors in related studies (e.g., Tajimi 1969, Roesset et al 1973, Pais and Kausel 1988).

METHOD OF ANALYSIS

Fundamental to the analysis presented here is the assumption that, under the horizontal excitation considered, no vertical normal stresses develop anywhere in the medium, i.e. $\sigma_z = 0$. It is further assumed that the horizontal variations of the vertical displacements of the medium w are negligible, such that the horizontal components of the shearing stresses can be expressed as

$$\tau_{zr} = G^* \frac{\partial u}{\partial z} \qquad \text{and} \qquad \tau_{z\theta} = G^* \frac{\partial v}{\partial z} \tag{1}$$

where u and v are the radial and tangential displacement components of the medium relative to the moving base; $G^* = G(1 + i\delta)$ is the complex-valued shear modulus; and $i = \sqrt{-1}$. The latter assumption implies that the cylinder-soil interface is smooth in the vertical direction, i.e., $\tau_{rz} = 0$. In the horizontal direction, however, the interface condition is considered to be either rough or smooth, i.e., either $v = 0$ or $\tau_{r\theta} = 0$. These assumptions are the same as those used by Arias et al (1981) in their study of straight walls.

Harmonic Response

For a harmonic input motion of acceleration

$$\ddot{x}_g(t) = \ddot{X}_g e^{i\omega t} \tag{2}$$

in which $\ddot{X}_g$ is the acceleration amplitude and ω the circular frequency of the motion, the steady-state radial and tangential displacements of the medium, u and v, may be expressed as

$$u(\xi, \theta, \eta, t) = \sum_{n=1}^{\infty} U_n(\xi) \sin\left[(2n-1)\frac{\pi}{2}\eta\right] \cos\theta \, e^{i\omega t} \tag{3}$$

$$v(\xi, \theta, \eta, t) = \sum_{n=1}^{\infty} V_n(\xi) \sin\left[(2n-1)\frac{\pi}{2}\eta\right] \sin\theta \, e^{i\omega t} \tag{4}$$

where $\xi = r/R$ and $\eta = z/H$ are dimensionless position coordinates; the sine functions represent the natural modes of vibration of the soil stratum when it is considered to act as series of vertical cantilever shear-beams; and U_n and V_n are the amplitudes of the modal components of the radial and circumferential displacements, defined by Eqs. (49) and (50) of Veletsos and Younan (1994b).* The method of analysis is similar to that employed by Tajimi (1969), except that Tajimi's solution is based on the assumption of vanishing vertical displacements rather than vanishing vertical normal stresses.

With the solution for u and v established, the radial normal pressures and circumferential shearing stresses at the cylinder-soil interface may be expressed in the form

$$\sigma_r(\theta, \eta, t) = -\rho \ddot{X}_g H \sum_{n=1}^{\infty} \sigma_n \sin\left[(2n-1)\frac{\pi}{2}\eta\right] \cos\theta \, e^{i\omega t} \tag{5}$$

$$\tau_{r\theta}(\theta, \eta, t) = \rho \ddot{X}_g H \sum_{n=1}^{\infty} \tau_n \sin\left[(2n-1)\frac{\pi}{2}\eta\right] \sin\theta \, e^{i\omega t} \tag{6}$$

* For the assumption of vanishing vertical normal stresses considered here, the factors ψ_e and ψ_σ should be replaced by the factor $\psi_o = \sqrt{2/(1-\nu)}$.

where σ_n and τ_n are complex-valued dimensionless factors that follow from Eqs. (59) and (60) of Veletsos and Younan (1994b).* These factors depend on the modal order n, Poisson's ratio ν, the material damping factor δ, and the dimensionless frequency parameter ω/ω_1. The quantity ω_1 represents the fundamental circular natural frequency of the soil layer when it is considered to act as a vertical cantilever shear-beam, and it is given by

$$\omega_1 = \frac{\pi}{2}\frac{v_s}{H} \tag{7}$$

where $v_s = \sqrt{G/\rho}$ is the shear wave velocity of the layer. The instantaneous values of the shear at the base of the cylinder, $Q_b(t)$, and of the corresponding moment, $M_b(t)$, are finally found by integration to be

$$\begin{aligned} Q_b(t) &= RH \int_0^1 \int_0^{2\pi} [\sigma_r \cos\theta - \tau_{r\theta} \sin\theta] \, d\theta \, d\eta \\ &= -\pi\rho \ddot{X}_g RH^2 \left[\frac{2}{\pi} \sum_{n=1}^{\infty} \frac{1}{2n-1} [\sigma_n + \tau_n] e^{i\omega t}\right] \end{aligned} \tag{8}$$

$$\begin{aligned} M_b(t) &= RH^2 \int_0^1 \int_0^{2\pi} [\sigma_r \cos\theta - \tau_{r\theta} \sin\theta] \, \eta \, d\theta \, d\eta \\ &= -\pi\rho \ddot{X}_g RH^3 \left[\frac{4}{\pi^2} \sum_{n=1}^{\infty} \frac{(-1)^{n-1}}{(2n-1)^2} [\sigma_n + \tau_n] e^{i\omega t}\right] \\ &= Q_b(t) h \end{aligned} \tag{9}$$

where h, referred to as the effective height, represents the height at which the total wall force or base shear should be considered to be concentrated to yield the correct base moment.

Transient Excitation

With the harmonic response established, the response to an arbitrary transient excitation may be evaluated by Fourier transform techniques.

STATIC RESPONSE OF SYSTEM

It is desirable to begin by examining the responses obtained for harmonic excitations the frequencies of which are small compared to the fundamental natural frequency of the stratum (i.e., for values of $\omega/\omega_1 \to 0$). Such excitations and the resulting effects will be referred to as *static*, a term that *should not be confused* with that normally used to represent the effects of gravity forces.

Fig. 3 shows the heightwise variations of the amplitudes of the normal pressures and circumferential shearing stresses

induced on the cylinder for systems with a rough interface and values of $H/R = 0$ and 3. These plots are normalized to unit values at the top. The variations for the intermediate values of H/R fall between those displayed and are not presented. The stress amplitudes increase almost as a quarter-sine wave from zero at the base to a maximum at the top, and are thus dominated by the fundamental mode of vibration of the layer. The same is also approximately true of the variations of the normal pressures for a smooth interface. The data displayed in the figure are for Poisson's ratio $\nu = 0.3$, a value, which except where otherwise indicated, is also used for the solutions presented in subsequent sections.

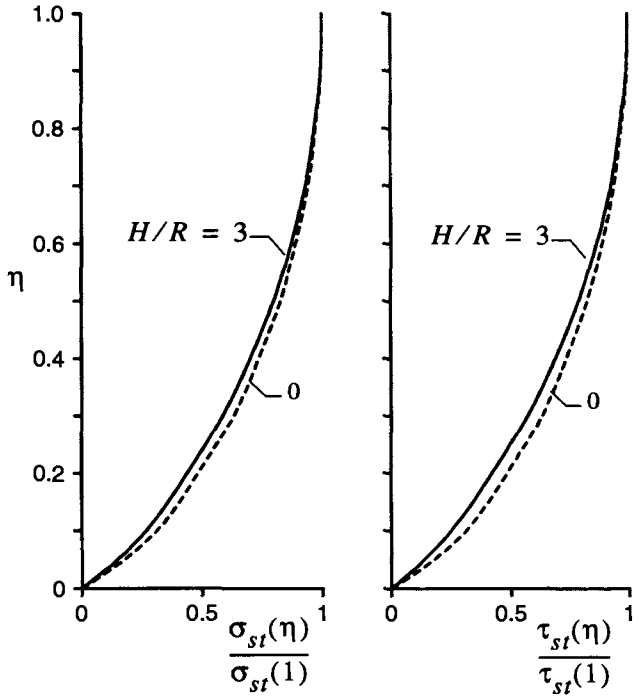

Fig. 3 Heightwise variations of static values of normal and circumferential wall stresses; rough interface, $\nu = 0.3$.

The maximum values of the static wall pressure, σ_{st}, and of the corresponding circumferential shearing stress, τ_{st}, attained at the top are shown in Fig. 4. These values are normalized with respect to the common multipliers of Eqs. (5) and (6), $\rho\ddot{X}_g H$, and are plotted as a function of the slenderness ratio, H/R. The solid lines in the figure define the stresses for a rough interface, whereas the dashed line defines the normal pressure for a smooth interface.

It is observed that: (1) both normalized stresses increase with increasing H/R; and (2) the normal pressure for the smooth interface is generally higher than for the rough, the difference becoming larger with increasing H/R. The first trend reflects the decreasing capacity of the deeper layers to transmit the inertia forces acting on them by horizontal shearing action to the base. The second trend is a consequence of

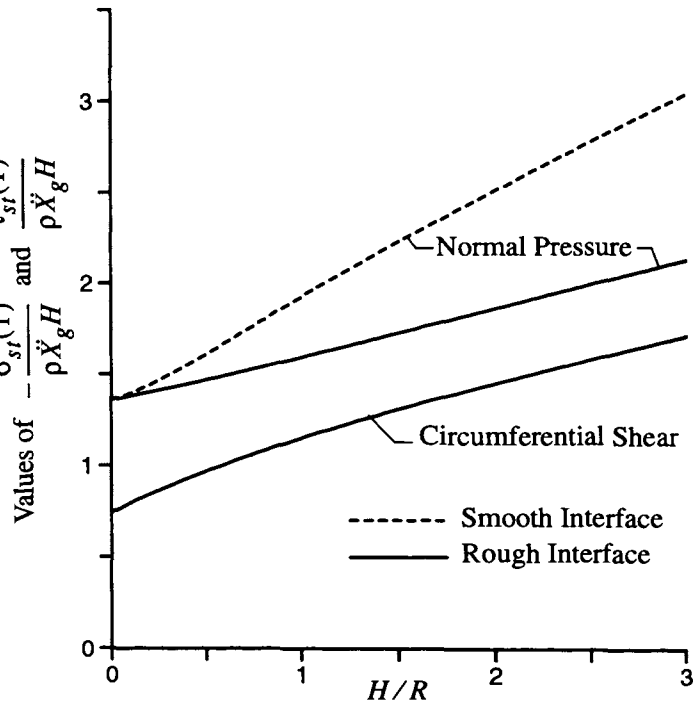

Fig. 4 Maximum values of normal and circumferential stresses; $\nu = 0.3$.

the ability of the rough interface to resist by circumferential shearing action a part of the force that gets transmitted to it. For a straight wall ($H/R \to 0$), the normal stress is naturally independent of the interface condition.

Unlike the normal wall pressures which have been shown to be generally smaller for the rough interface than for the smooth, the total force per unit of cylinder height should be larger for the rough interface. Being the 'stiffer' of the two, the rough interface would be expected to attract a higher proportion of the forces acting on the medium. That this is indeed the case is demonstrated in Fig. 5, in which the static value of the base shear, $(Q_b)_{st}$, is plotted as a function of H/R. The results in this case are normalized with respect to $\pi\rho\ddot{X}_g RH^2$, and are, as before, for a value of $\nu = 0.3$. Since the response of the system is governed by the fundamental mode of vibration of the layer, the corresponding results for the static base moment, $(M_b)_{st}$, are given approximately by the product of $(Q_b)_{st}$ and an effective height of $h = (2/\pi)H$. The exact values of the static base shear are listed in Table 1 for systems with different values of H/R and different interface conditions.

For the limiting case of a straight wall, $H/R \to 0$, the base shear per unit length, $Q_b'(t)$, is given by $Q_b(t)/(\pi R)$, and the base moment per unit of length, $M_b'(t)$, is given by $M_b(t)/(\pi R)$. Considering that these forces are induced only by normal pressures in this case, the relevant values in Table 1 are those corresponding to the smooth interface condition. For

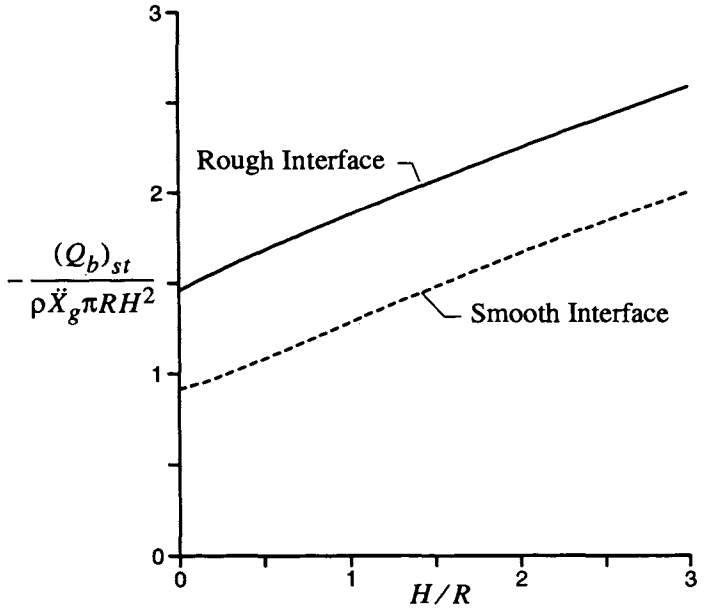

Fig. 5 Static values of total force or base shear for cylinder; $\nu = 0.3$.

the significance of the results for the rough interface as $H/R \to 0$, reference may be made to Veletsos and Younan (1994b).

Accuracy of Solution

Reference has already been made to Tajimi's solution (1969) which is based on the assumption of vanishing vertical displacements rather than of vanishing vertical stresses. As an indication of the interrelationship and relative accuracy of the solutions based on these two assumptions, the normalized static values of the base shear and base moment per unit of length for a straight wall computed by the two approaches are compared in Fig. 6 over a range of Poisson's ratios for the medium ν with those obtained by Wood's more rigorous solution (1973). It is observed that, while the results based on the assumption of vanishing normal vertical stresses are in very good agreement with the 'exact' results over the full range of ν values, the accuracy of the solution based on the assumption of vanishing vertical displacements deteriorates rapidly for values of $\nu \geq 1/3$ and ceases to be acceptable near the limiting value of $\nu = 1/2$.

Table 1: Static values of base shear for systems with different H/R ratios; $\nu = 0.3$.

H/R	$-\frac{(Q_b)_{st}}{\pi\rho\ddot{X}_g RH^2}$		H/R	$-\frac{(Q_b)_{st}}{\pi\rho\ddot{X}_g RH^2}$	
	Rough	Smooth		Rough	Smooth
0	1.459	0.918	1.25	1.973	1.382
0.30	1.595	1.005	1.50	2.065	1.478
0.40	1.638	1.042	1.75	2.156	1.571
0.50	1.679	1.081	2.00	2.245	1.661
0.60	1.720	1.122	2.50	2.418	1.835
0.70	1.760	1.162	3.00	2.585	2.001
0.80	1.800	1.203	5.00	3.214	2.612
1.00	1.878	1.283	10.00	4.616	3.942

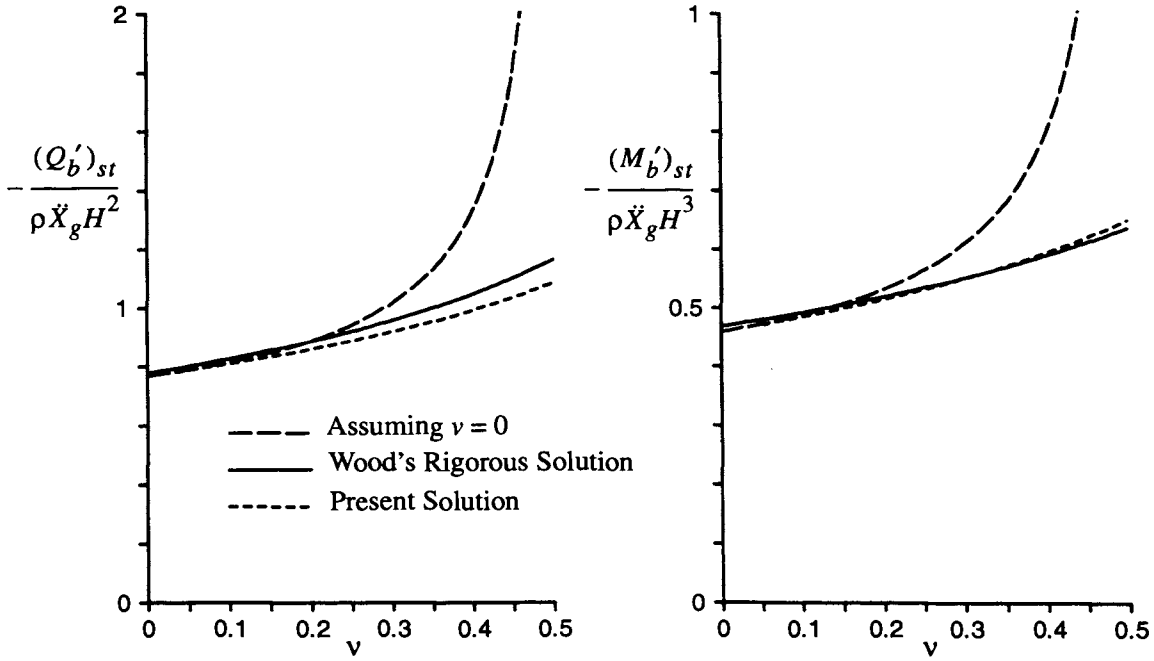

Fig. 6 Comparison of static values of base shear and base moment in straight wall obtained by different approaches; $\nu = 0.3$.

DYNAMIC RESPONSE OF SYSTEM

Harmonic Response

Figure 7 shows the variation with the frequency ratio ω/ω_1 of the components of the base shear, Q_b', induced in a straight wall by a harmonic excitation. Normalized with respect to $\rho\ddot{X}_g H^2$, the results are for a medium with $\nu = 0.3$ and $\delta = 0.1$. The solid line defines the real part of the force, whereas the dashed line defines the imaginary part. The real part is, of course, in phase with the exciting motion and represents the restraining effect of a displacement-proportional, spring-like action of the medium, whereas the imaginary part is 90° out of phase and represents the effect of a damping mechanism analogous to that of a viscous damper. The following trends are worth noting:

1. For $\omega = 0$, the imaginary part of the base shear vanishes, and the real part reduces, as it should, to $0.918\rho\ddot{X}_g H^2$, the value of the static shear for the smooth interface listed in Table 1.
2. For values of $\omega/\omega_1 < 1$, the force amplitude is dominated by the real part, whereas for $\omega/\omega_1 \geq 1$, it is dominated by the imaginary part. Note, in particular, the very rapid and large increase of the imaginary part in the neighborhood of $\omega = \omega_1$. The relative unimportance of the imaginary part for $\omega/\omega_1 < 1$ is due to the fact that no energy gets dissipated by radiation of waves within this frequency range.

The real-valued amplitude of the base shear, $|Q_b'|$, which is given by the square root of the sum of the squares of the real and imaginary parts displayed in Fig. 7, is plotted in Fig. 8 as a function of the frequency ratio ω/ω_1. The results are again normalized with respect to $\rho\ddot{X}_g H^2$ and are given for a medium with $\nu = 0.3$ and $\delta = 0.1$. The dashed line defines the solution obtained by the present approach, whereas the solid line defines Wood's more rigorous solution (1973). It should be noted that Wood's solution is strictly applicable to a stratum that is retained by a pair of vertical walls located a distance L apart, rather than to the semi-infinite layer examined here. Furthermore, his solution requires consideration of a large number of terms and must be evaluated with extreme care as it may lead to numerical instabilities. For the solutions presented here, the distance between walls was taken as $L = 50H$, and the relevant series expression was evaluated using 270 terms and following the computational guidelines specified by Wood. The agreement between the two solutions is quite satisfactory. Note that the maximum base shear is attained at $\omega = \omega_1$ and that it is associated with an amplification factor of 3.05. The latter value is close to the value of 3.16 defined by the expression $1/\sqrt{\delta}$ and significantly different from the value of 10 obtained from the expression $1/\delta$ governing the resonant response of a viscously damped simple oscillator with a fraction of critical damping $\beta = \delta/2$. This fact has been noted previously by Arias et al (1981).

The effect of material damping on the frequency response curves for base shear in straight walls is displayed in Fig. 9.

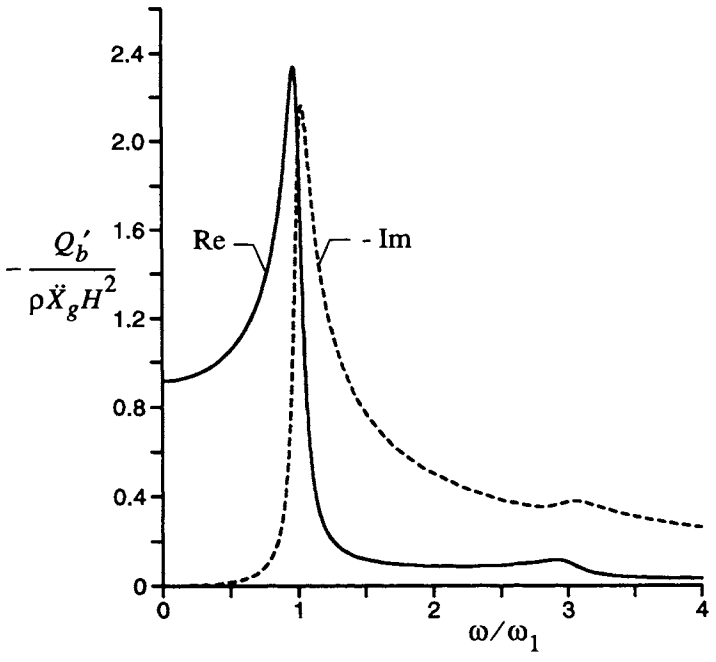

Fig. 7 Frequency response curves for base shear in straight walls; $\nu = 0.3$ & $\delta = 0.1$.

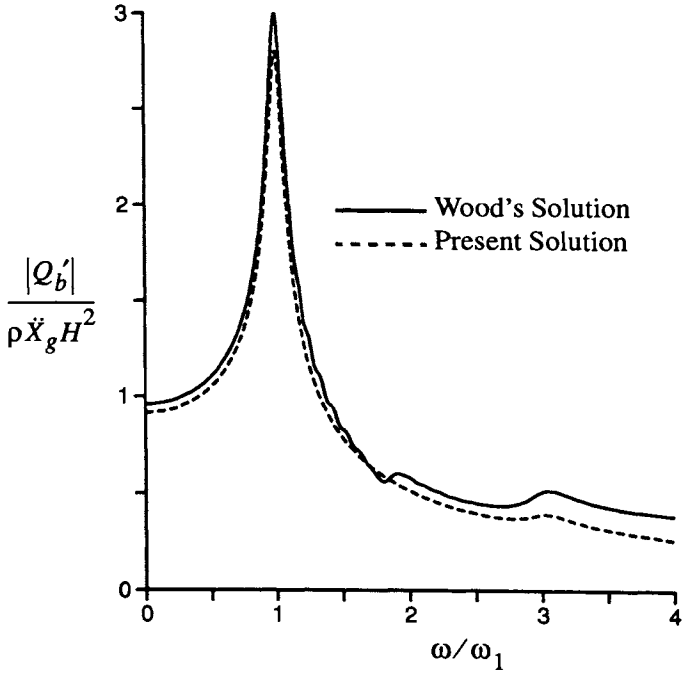

Fig. 8 Frequency response curves for base shear amplitude in straight walls; $\nu = 0.3$ & $\delta = 0.1$.

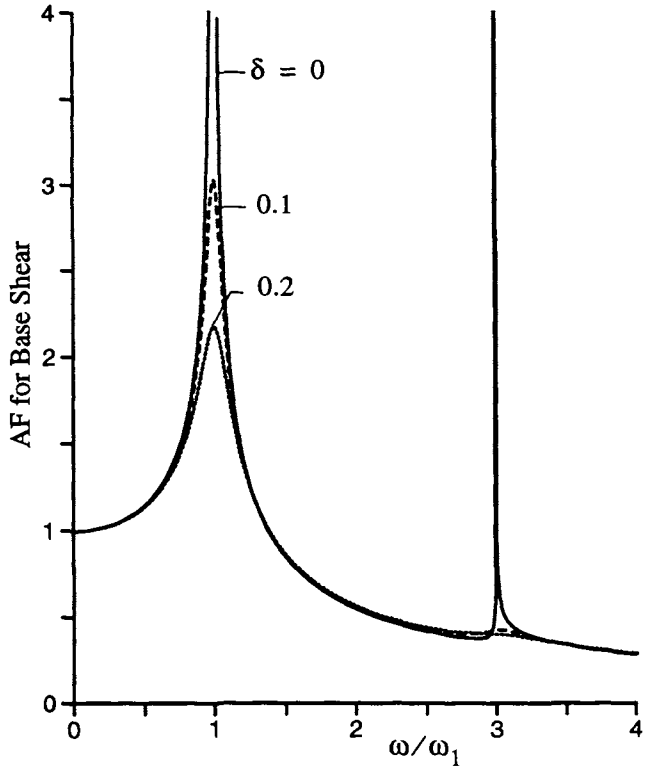

Fig. 9 Effect of material damping on frequency response curves for base shear in straight walls; $\nu = 0.3$.

Poisson's ratio for the medium is again taken as $\nu = 0.3$. The amplification factors start at the left from unity, and the curve for the undamped system becomes infinite at exciting frequencies equal to the natural frequencies of the layer. Soil material damping reduces significantly the resonant peaks, particularly those corresponding to the higher modes of vibration. The very significant effect of damping on the higher resonant peaks along with the general trends of the displayed curves indicate that, except for the totally undamped systems which are of no practical interest, the fundamental mode of vibration of the stratum is the dominant contributor to the response of the system.

The maximum amplification factors for base shear in systems with different values of H/R and δ are displayed in Fig. 10. The results are for a medium with $\nu = 0.3$. The solid lines in this figure are for systems with a rough interface, whereas the broken lines are for systems with a smooth interface. It is observed that the amplification factors increase more rapidly with H/R for the smooth interface than for the rough. This is attributed to the fact that, whereas the smooth interface can radiate only compressional waves, the rough interface can radiate both compressional and horizontally polarized shear waves. Accordingly, systems with a rough interface have higher damping capacities and lower resonant peaks than those with a smooth interface.

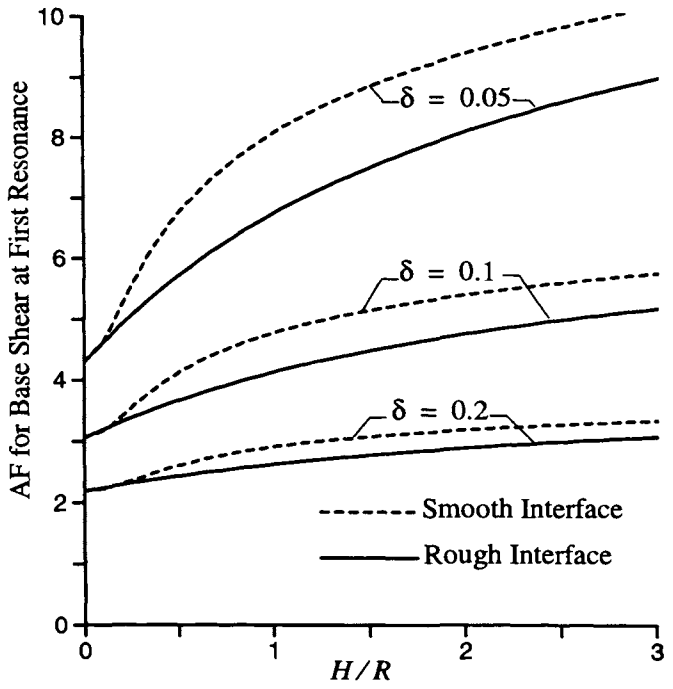

Fig. 10 Effect of slenderness ratio & material damping on resonant amplification factor for base shear; $\nu = 0.3$.

Solutions for Transient Response

The response of the medium was also evaluated for the first 6.3 sec of the N-S component of the ground motion recorded during the 1940 El Centro, California earthquake. The acceleration, velocity and displacement traces of this record have been presented before (Veletsos and Tang 1990). The peak value of the ground acceleration is $\ddot{x}_g = 0.312g$, and the corresponding values of the velocity and displacement are $\dot{x}_g = 14.02$ in/sec and $x_g = 8.29$ in.

The solid lines in Fig. 11 define the amplification factors for the absolute maximum base shear induced by the El Centro ground motion in a fully bonded cylinder with different values of H/R and medium properties defined by $\nu = 0.3$ and $\delta = 0.1$. The static values of the base shear involved in the definition of this factor are listed in Table 1, in which $\ddot{X}_g$ must now be interpreted as the maximum ground acceleration of the transient ground motion. The results are plotted as a function of the fundamental period of the system, defined by

$$T_1 = \frac{4H}{v_s} \tag{10}$$

As a measure of the values of T_1 that may be encountered in practice, it should be noted that for values of v_s in the range between 400 and 1600 ft/sec and values of H in the range between 20 and 50 ft, the value of T_1 falls in the range between 0.05 to 0.5 sec.

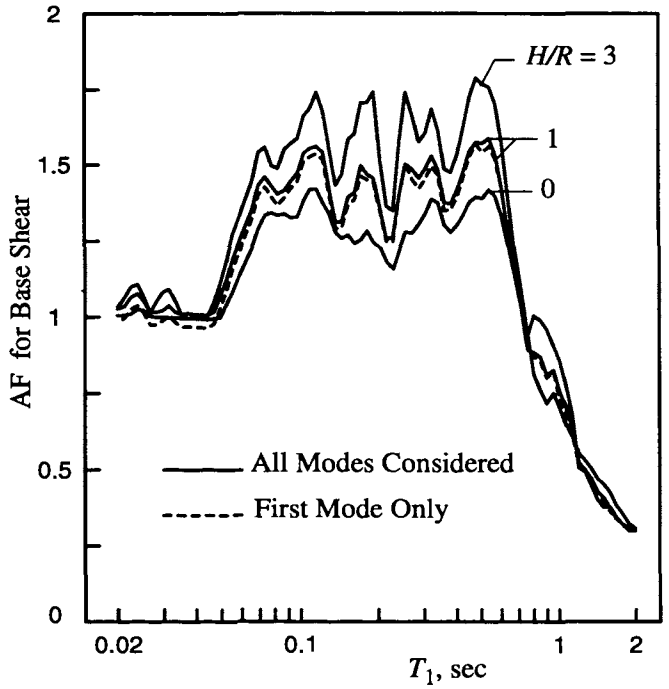

Fig. 11 Amplification factors for base shear due to El Centro record; rough interface, $\nu = 0.3$ & $\delta = 0.1$.

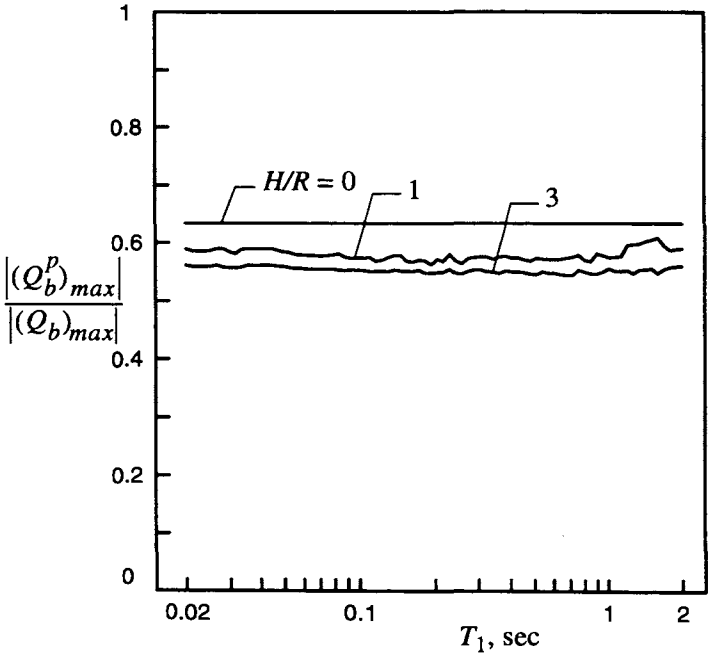

Fig. 12 Portion of maximum base shear contributed by pressures; rough interface, $\nu = 0.3$ & $\delta = 0.1$.

For very stiff strata with values of T_1 of the order of 0.05 sec or less, the amplification factors in Fig. 11 are effectively unity, and the maximum base shears reduce to the values listed in Table 1. As the system period increases, the amplification factors generally increase, the increase being more or less proportional to the value of the slenderness ratio, H/R. For highly compliant systems with very high natural periods, the amplification factors are naturally less than unity.

The dashed curve in Fig. 11 defines the amplification factors computed for a system with $H/R = 1$ considering the contribution of only the fundamental mode of vibration of the medium. As anticipated from the responses of harmonically excited systems examined earlier, the agreement with the more nearly exact solution is indeed excellent. It follows that even for the fairly complex ground shaking considered, the maximum values of the wall forces may, for all practical purposes, be considered to increase as a quarter-sine wave from zero at the base to a maximum value at the top, and the maximum base moment may be computed as the product of the maximum base shear and the height $h = 0.637H$.

As a measure of the relative contribution to the maximum base shear of the interfacial normal pressures, σ_r, and of the corresponding circumferential shearing stresses, $\tau_{r\theta}$, the component induced by the normal pressures, $(Q_b^p)_{max}$, is plotted in Fig. 12 as a fraction of the corresponding total base shear, $(Q_b)_{max}$, for systems with different values of H/R and T_1 subjected to the El Centro record. It is observed that this ratio is insensitive to variations in both H/R and T_1. In other words, irrespective of the excitation and the characteristics of the system, approximately 60 percent of the base shear and base moment in cylinders with rough interface may be considered to be caused by the normal pressures, with the remaining 40 percent caused by the circumferential shearing stresses.

MODELING OF SYSTEM

Scott's Model

Probably the simplest available approximate model for evaluating the dynamic soil pressures induced by ground shaking on straight walls retaining an elastic stratum is the one proposed by Scott (1973). Proposed originally for a stratum of finite width retained by a straight vertical wall at each end, the model is also applicable to the important limiting case of the semiinfinite stratum considered here.

Scott's model for the semiinfinite stratum is shown in Fig. 13. It consists of a vertical cantilever shear-beam that simulates the far-field action of the stratum, and a set of massless, linear horizontal springs connecting the shear-beam to the wall. The height and material properties of the beam are taken equal to those of the stratum, and the stiffness of the springs per unit of length and height of the wall, K', is taken as

$$K' = \frac{0.8(1-\nu)}{1-2\nu}\frac{G}{H} \tag{11}$$

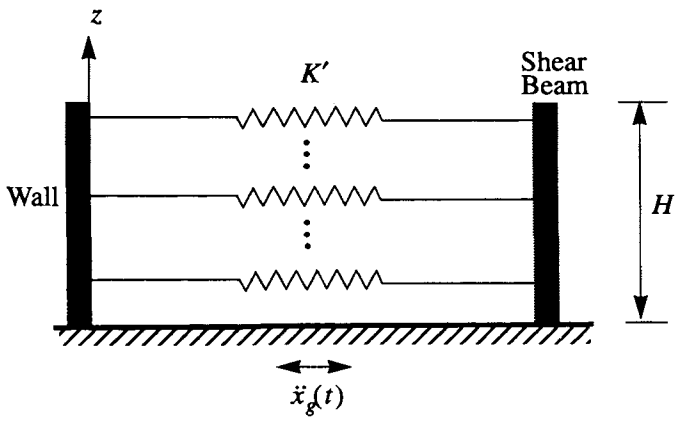

Fig. 13 Scott's model

This stiffness is the same as the static extensional stiffness of a bar of unit cross-sectional area and length $2.5H$ that is constrained along its sides against both lateral and vertical displacements. The bases of both the shear-beam and the wall in the model are presumed to be excited by the same ground motion.

Let u_f be the free-field displacement relative to the moving base of a point in the medium located at a dimensionless distance η from the base. For the harmonic input motion defined by Eq. (2), this displacement is of the form

$$u_f(\eta, t) = \sum_{n=1}^{\infty} U_{fn} \sin\left[(2n-1)\frac{\pi}{2}\eta\right] e^{i\omega t} \qquad (12)$$

and the corresponding wall pressure at that level is given by the product of K' and the relative motions of the shear-beam and the wall at that level, i.e.,

$$\sigma(\eta, t) = K' u_f = K' \sum_{n=1}^{\infty} U_{fn} \sin\left[(2n-1)\frac{\pi}{2}\eta\right] e^{i\omega t} \qquad (13)$$

The corresponding base shear and base moment are then found by integration to be

$$Q_b'(t) = \frac{2}{\pi} K' H \sum_{n=1}^{\infty} \frac{1}{2n-1} U_{fn} e^{i\omega t} \qquad (14)$$

$$M_b'(t) = \frac{4}{\pi^2} K' H^2 \sum_{n=1}^{\infty} \frac{(-1)^{n-1}}{(2n-1)^2} U_{fn} e^{i\omega t} \qquad (15)$$

Note that the spring stiffness is independent of the characteristics of the ground motion and that the only damping for the model is that involved in the shear-beam itself. Note further that as $\nu \to 0.5$, K' and hence the wall pressures and associated forces become infinite, a result that is clearly unacceptable.

Scott's model has been used extensively (e.g., Karkanias 1983, Dennehy 1984, Jain and Scott 1989, Alampalli and Elgamal 1991, Soydemir 1991), and variations of it, involving combinations of springs and dashpots with frequency-dependent parameters, have been used in analyses of embedded foundations (Beredugo and Novak 1972, Novak and Beredugo 1972), piles (Novak 1974, Flores-Berrones and Whitman 1982) and underground cylindrical structures (Miller et al 1991).

As a measure of the accuracy of this model, a comparison is made in Fig. 14 of the amplitudes of the steady-state shear at the base of the wall, $|Q_b'|$, computed for harmonically excited systems by this approach and by the nearly exact solution presented herein. The latter solution is represented by the solid line curve, whereas Scott's solution is represented by the curve in short dashed lines. The significance of the remaining curve is discussed in later sections. Poisson's ratio and the material damping factor for the medium are taken again as $\nu = 0.3$ and $\delta = 0.1$. The results are normalized with respect to $\rho \ddot{X}_g H^2$ and are plotted against the frequency ratio ω/ω_1. The agreement between the two sets of solutions is clearly not satisfactory. Note in particular that, whereas the present solution leads to significantly larger base shears than Scott's solution at the low and high values of the frequency ratio, the opposite is true for values of ω/ω_1 close to unity.

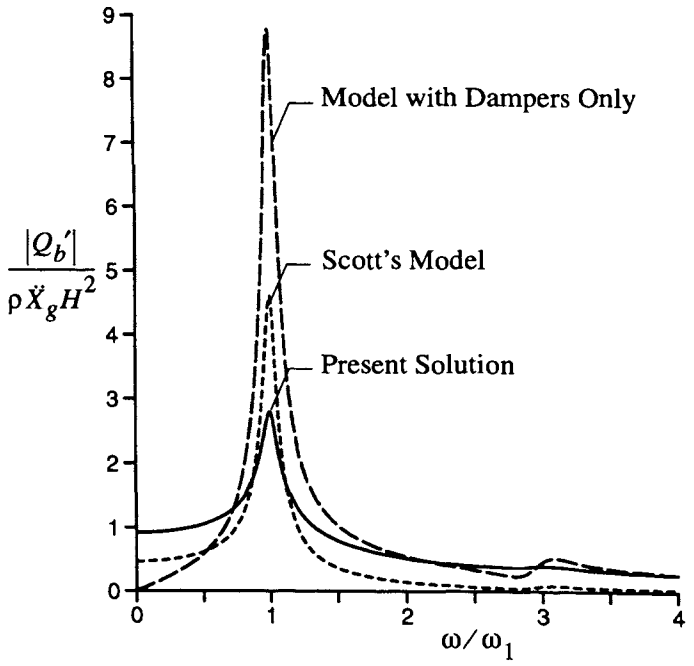

Fig. 14 Frequency response curves for base shear amplitude in straight walls; $\nu = 0.3$ & $\delta = 0.1$.

Modification of Scott's Model

The discrepancies in Scott's solution are due, in part, to the failure of the model to provide for the radiational capacity of the medium. If instead of a series of massless, horizontal linear springs of constant stiffness simulating the action of the massless bars of finite length shown in Fig. 15(a), the medium were approximated by a series of infinitely long bars of finite mass per unit of length, as shown in Fig. 14(b), it is well known (Wolf 1988) that the action of the latter bars for a harmonic base motion would be identical to that of a series of dashpots. On the assumption that the bars are constrained laterally and that their horizontal faces are stress free, the equivalent damping coefficient of the dashpots, c, is given by

$$c = \sqrt{\frac{2}{1-\nu}G\rho} \tag{16}$$

The curve in long dashed lines in Fig. 14 represents the frequency response curve for the base shear in the wall computed on the assumption that the medium can be modeled by a series of horizontal dashpots rather than by massless springs. It is observed that, while at high values of the frequency parameter, the latter modeling of the medium is definitely superior to that of Scott, it too leads to unacceptable results in the lower frequency range.

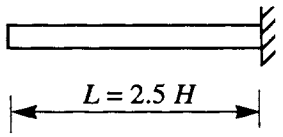

(a) Massless Bar - - Constrained Vertically & Laterally

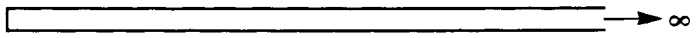

(b) Semi-Infinite Bar with Distributed Mass - - Laterally Constrained

Fig. 15 Representation of soil-stratum in Scott's model and its variant.

Proposed Model for System with Straight Wall

Both models referred to above are deficient in that they fail to provide for the capacity of the medium between the wall and the far field to transfer forces vertically by horizontal shearing action. In addition to the horizontal normal stresses and inertia forces, a horizontal element of the medium is acted upon along its upper and lower faces by horizontal shearing stresses, as shown in Fig. 16(a). It can be shown (Veletsos and Younan 1994c) that, when the stratum is vibrating in its nth natural mode, the effect of these shearing stresses may be represented by a set of horizontal linear springs of stiffness k_n,

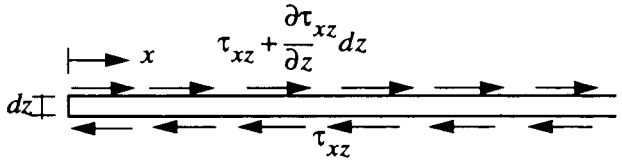

(a) State of Shearing Stresses

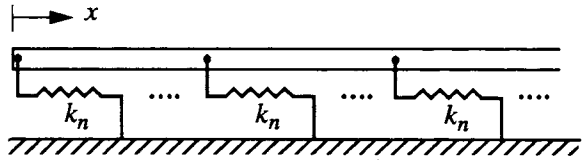

(b) Elastically Constrained Bar (Laterally Constrained)

Fig. 16 Exact modeling of soil-stratum

defined by

$$k_n = \rho\omega_n^2 = \left[\frac{(2n-1)\pi}{2}\right]^2 \frac{G}{H^2} \tag{17}$$

in which ω_n is the nth natural frequency of the stratum given by

$$\omega_n = (2n-1)\frac{\pi}{2}\frac{v_s}{H} \tag{18}$$

It follows that, within the confines of the simplified method of analysis considered here, the medium can be modeled correctly by a series of semiinfinitely long, elastically supported horizontal bars with distributed mass, as shown in Fig. 16(b). The lower ends of all these springs should be attached to the common moving base.

Bar Stiffness. The evaluation of the dynamic response of a semiinfinitely long, elastically supported bar of uniform mass density is a fundamental problem in foundation dynamics that has already been addressed in the literature (Wolf 1988). Defined for a bar in harmonic motion, the dynamic stiffness or impedance of the bar, K_n', represents the amplitude of the harmonic end force necessary to induce a steady-state end displacement of unit amplitude. This is a complex-valued quantity that depends on the characteristics of the bar and the frequency of excitation. For a viscoelastic bar with frequency-independent damping

$$K_n' = \frac{(2n-1)\pi}{\sqrt{2(1-\nu)}}\frac{G}{H}\left[\alpha_n' + i\frac{\omega}{\omega_n}\beta_n'\right] \tag{19}$$

where α_n' and β_n' are dimensionless stiffness and damping coefficients that depend on the frequency ratio ω/ω_n and the material damping factor δ.

Figure 17 shows the variations of α_n' and β_n' as a function of the frequency ratio ω/ω_n for several values of the damping factor δ. Also shown for the special case of an undamped medium are the corresponding values obtained by Scott's model for values of $n = 1$ and $\nu = 0.3$. There is clearly lack of agreement between the results obtained by the latter model and by the proposed, practically exact model.

Response of System. With the impedance of the bar established, the steady-state wall pressures and the associated forces may be computed in the spirit of Eqs. (13)-(15) as

$$\sigma(\eta, t) = \sum_{n=1}^{\infty} K_n' U_{fn} \sin\left[(2n-1)\frac{\pi}{2}\eta\right] e^{i\omega t} \qquad (20)$$

$$Q_b'(t) = \frac{2}{\pi} H \sum_{n=1}^{\infty} \frac{1}{2n-1} K_n' U_{fn} e^{i\omega t} \qquad (21)$$

$$M_b'(t) = \frac{4}{\pi^2} H^2 \sum_{n=1}^{\infty} \frac{(-1)^{n-1}}{(2n-1)^2} K_n' U_{fn} e^{i\omega t} \qquad (22)$$

Note that, unlike Eqs. (13) through (15), in which the impedance K' appears as a common multiplier, K_n' in Eqs. (20) through (22) appears under the summations and has values that are not only different from K' but are also different for different values of the modal order n.

The response of the system computed by this model is identical to that obtained by the nearly exact solution summarized in the first part of this paper.

Modeling of Cylindrical System

The concepts underlying Scott's model have also been applied to the analysis of cylindrical systems making use of the Baranov-Novak (B-N) idealization for the medium (Baranov 1967, Beredugo and Novak 1972, Novak 1974, Miller et al 1991). In this approach, the soil is modeled by a series of independent thin layers with a circular hole at the center, and their resistance to deformation is expressed by their impedance, defined as the complex-valued amplitude of a harmonic force which when applied along the inner circular boundary in the direction of the desired response will induce a steady-state displacement of unit amplitude in that direction.

The impedance of a horizontally excited B-N layer, K, may be conveniently be expressed in the form suggested by Veletsos and Dotson (1988) as

$$K = 1.5\pi G[\alpha + ia_o\beta] \qquad (23)$$

where $a_o = \omega R/v_s$ is a dimensionless frequency parameter; and α and β are dimensionless factors that depend on a_o, Poisson's ratio for the medium ν, and the associated material damping factor δ.

B-N Modeling. Under the influence of the ground motion, the thin cylindrical element of the medium at the far-field shown shaded in the upper part of Fig. 18 will respond as a uniform, cantilever shear-beam. The stratum may then be modeled by a shear-beam at the far-field and by a series of B-N layers between the shear-beam and the cylinder, as shown in the lower part of the figure.

For the harmonic input motion defined by Eq. (2), the force per unit of cylinder height, $F(\eta, t)$, and the correspond-

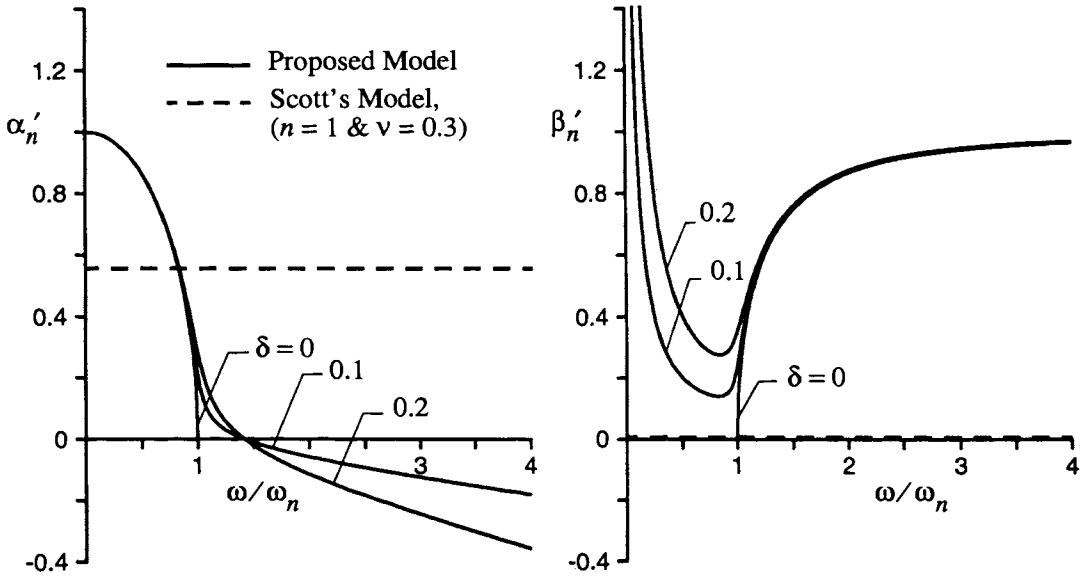

Fig. 17 Stiffness and damping factors for elastically constrained bar; straight wall.

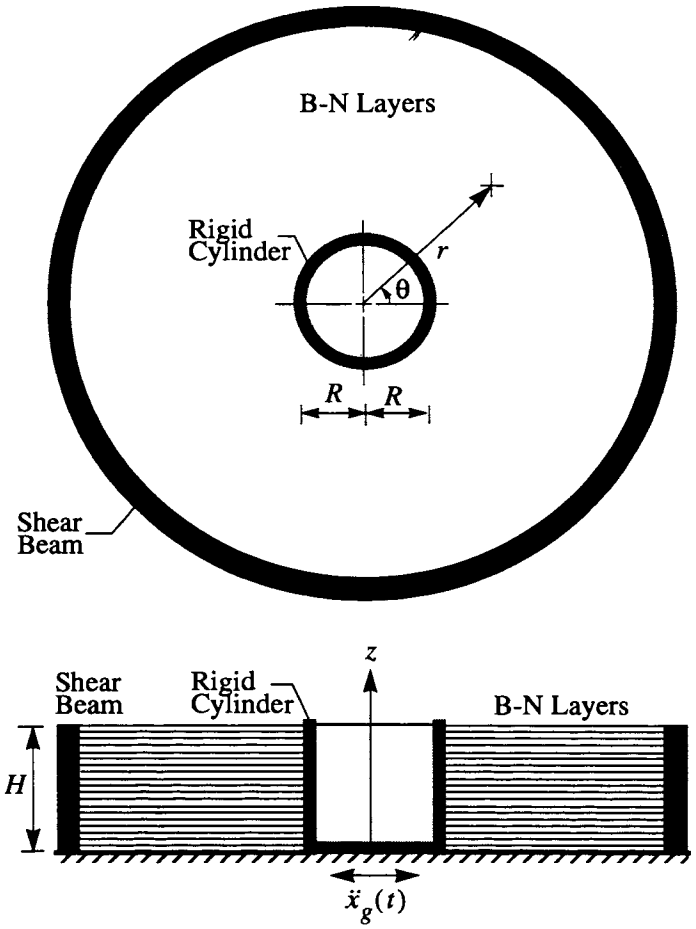

Fig. 18 Model for system with embedded cylinder

ing base shear and base moment, $Q_b(t)$ and $M_b(t)$, may be expressed in forms analogous to Eqs. (13)-(15) as

$$F(\eta, t) = Ku_f = K\sum_{n=1}^{\infty} U_{fn}\, sin\left[(2n-1)\frac{\pi}{2}\eta\right]e^{i\omega t} \quad (24)$$

$$Q_b(t) = \frac{2}{\pi}KH\sum_{n=1}^{\infty}\frac{1}{2n-1}U_{fn}e^{i\omega t} \quad (25)$$

$$M_b(t) = \frac{4}{\pi^2}KH^2\sum_{n=1}^{\infty}\frac{(-1)^{n-1}}{(2n-1)^2}U_{fn}e^{i\omega t} \quad (26)$$

It should be clear that this model, like the corresponding model for the stratum retained by a straight wall, also suffers from its failure to account for the capacity of the medium between the cylinder and the far field to transfer forces vertically by horizontal shearing action.

Proposed Modeling. Following the reasoning used in the analysis of the system with a straight wall, it can be shown (Veletsos and Younan 1995) that the cylindrical system can be modeled by a series of elastically supported thin layers as shown in Fig. 19. The individual layers in this case are elastically constrained both radially and circumferentially by a series of massless linear springs, the stiffness of which in each direction and for each modal component of response is also defined by Eq. (17).

The impedance of the elastically supported layer when vibrating in its nth natural mode, K_n, may then be expressed (Veletsos and Younan 1995) in a form analogous to Eq. (23) as

$$K_n = 1.5\pi G[\alpha_n + ia_o\beta_n] \quad (27)$$

in which the dimensionless factors α_n and β_n are now functions not only of a_o, ν and δ, but also of the dimensionless measure of the stiffness of the supporting springs

$$s_n = \sqrt{\frac{k_n R^2}{G}} = (2n-1)\frac{\pi}{2}\frac{R}{H} \quad (28)$$

The variations of α_n and β_n as a function of the frequency parameter a_o are shown in Fig. 20 for an undamped layer with $\nu = 0.3$. Four values of s_n in the range between zero and π are considered which, for $n = 1$, correspond to the H/R values shown in parentheses. As would be expected, the results for $s_n = 0$, shown in dashed lines, are identical to those for the B-N layer, but those for the finite values of s_n are substantially different, particularly for the smaller values of a_o and H/R.

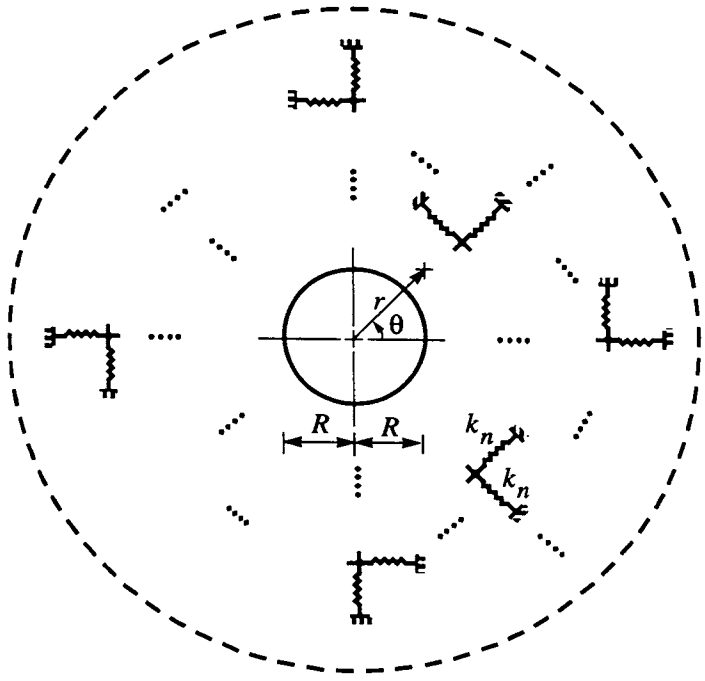

Fig. 19 Elastically constrained thin layer

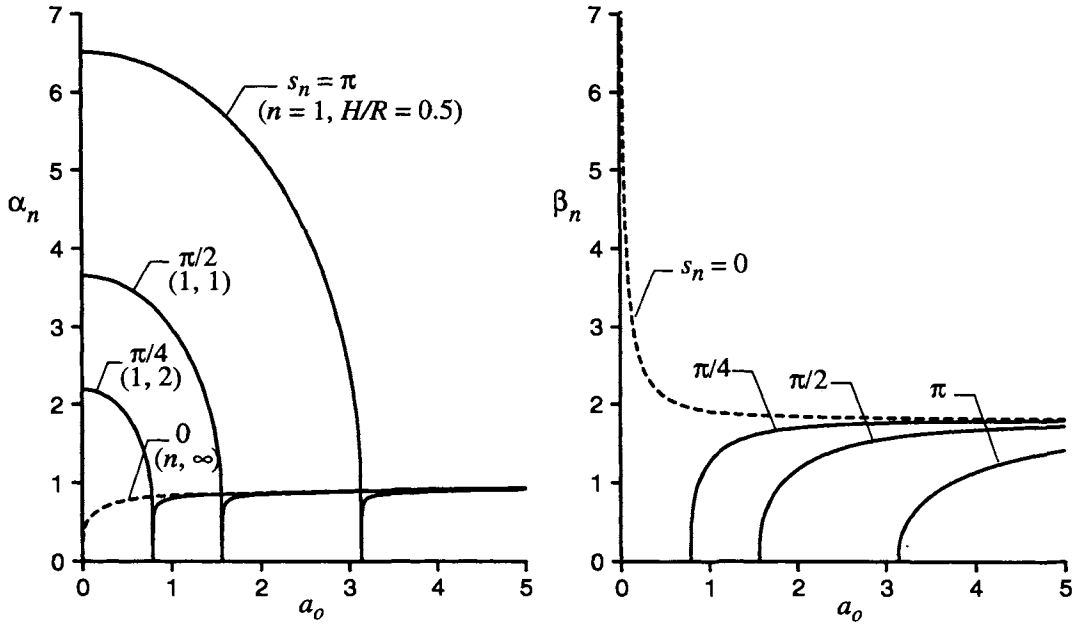

Fig. 20 Stiffness and damping factors for elastically constrained thin layer; $\nu = 0.3$, $\delta = 0$.

For the values of a_o corresponding to the natural frequencies of the stratum defined by Eq. (18), the stiffness factors $\alpha_n = 0$, and for the smaller values of a_o, the damping factors $\beta_n = 0$. The latter result is consistent with the well established fact that the stratum possesses no radiational damping capacity within this frequency range. For values of a_o greater than those corresponding to the natural frequencies of the stratum, both the factors α_n and the factors β_n for the elastically constrained layer are in close agreement with those for the unconstrained layer. It follows that the conventional modeling of the stratum by unconstrained B-N layers would be sufficiently accurate for this range of a_o values, but this clearly would not be true for the lower values of a_o.

With the modal impedances established, the dynamic force per unit of cylinder height and the associated base shear and base moment may be obtained from Eqs. (20)-(22) merely by replacing K_n' by K_n. The results in this case will be identical to those obtained by the method of analysis summarized in the early part of this paper.

Response of System. Figure 21 shows the real-valued amplitude of the base shear for the cylinder of harmonically excited systems with four different values of H/R in the range between 0.3 and 10. The solid lines represent the solutions obtained by the proposed approach using the elastically supported layers, whereas the dashed lines represent those obtained using the unconstrained B-N layers. The results are expressed in the form of amplification factors (i.e., they are normalized with respect to the corresponding static shears listed in Table 1), and they are plotted as a function of the frequency ratio ω/ω_1. Poisson's ratio for the medium ν and the associated material damping factor δ in these solutions are taken as 0.3 and 0.1, respectively. It can be seen that the results obtained with the unconstrained B-N layers may differ significantly from the practically exact results obtained with the constrained layers, the differences being particularly large for the smaller values of H/R. The smaller the H/R, the greater is the horizontal shearing stiffness of the medium relative to its extensional stiffness, the greater is the proportion of the load transmitted by horizontal shearing action to the base, and, therefore, the less accurate is the modeling of the medium by the conventional, unconstrained B-N layers. For very slender cylinders such as piles, practically the entire load gets transmitted by extensional action, and the conventional B-N approach, as already demonstrated by Nogami and Novak (1977), does yield highly accurate results. This is clearly not the case, however, for the broader systems with relatively small H/R values.

The interrelationship of the two sets of solutions also depends on the frequency ratio ω/ω_1. At low values of ω/ω_1, for which the impedance of the unconstrained B-N layers tends to zero, the conventional approach leads to unacceptably low base shears. By contrast, at high values of ω/ω_1, the two solutions are in a very good agreement; high frequency waves are clearly transmitted by extensional action, and it is immaterial in this case whether the soil layers are considered to be constrained or not. The differences between the two solution sets are most pronounced in the intermediate

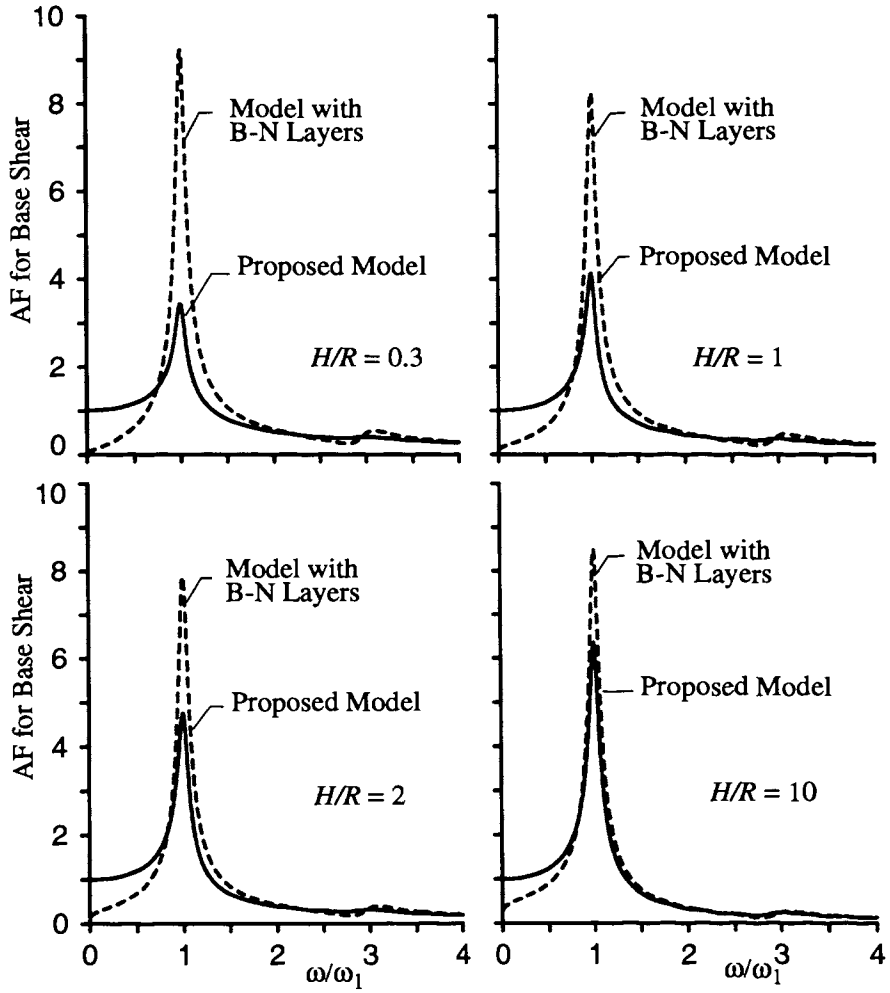

Fig. 21 Frequency response curves for amplitude of base shear in harmonically excited systems; $\nu = 0.3$, $\delta = 0.1$

range of frequencies, especially for exciting frequencies that are close to the fundamental natural frequency of the stratum.

Precisely the same trends are also observed in Fig. 22, which defines the amplification factors for base shear in the cylinder induced by the first 6.3 sec of the N-S component of the 1940 El Centro, California earthquake ground motion.

CONCLUSIONS

With the expressions summarized in the first part of this paper, the dynamic pressures and associated forces induced by horizontal ground shaking on a rigid vertical cylinder embedded in a stratum, or on a straight wall retaining such a stratum, may be evaluated reliably and cost-effectively. The numerical data that have been presented provide not only valuable insights into the responses of these systems and into the effects and relative importance of the numerous parameters involved, but also a conceptual framework for the analysis and interpretation of the solutions for much more complex systems as well.

The representation of the soil stratum by a series of independent massless springs as proposed by Scott for straight walls, and by a series of unconstrained Baranov-Novak layers for embedded cylinders may lead to major inaccuracies. These inaccuracies stem from the failure of these representations to provide for the capacity of the medium between the structure and the far field to transfer forces vertically by horizontal shearing action. The greater the horizontal shearing stiffness of the medium relative to its horizontal extensional stiffness, the greater are generally the resulting discrepancies. This deficiency in modeling may be eliminated by considering the individual soil layers to be elastically supported on the common oscillating base.

The data presented herein are for straight or cylindrical walls that are rigid and for a non-deformable moving base. The presence of a flexible rather than a rigid wall will reduce the effective horizontal extensional stiffness of the medium relative to its shearing stiffness, and this reduction, in turn, will increase the forces that get transmitted to the base by hor-

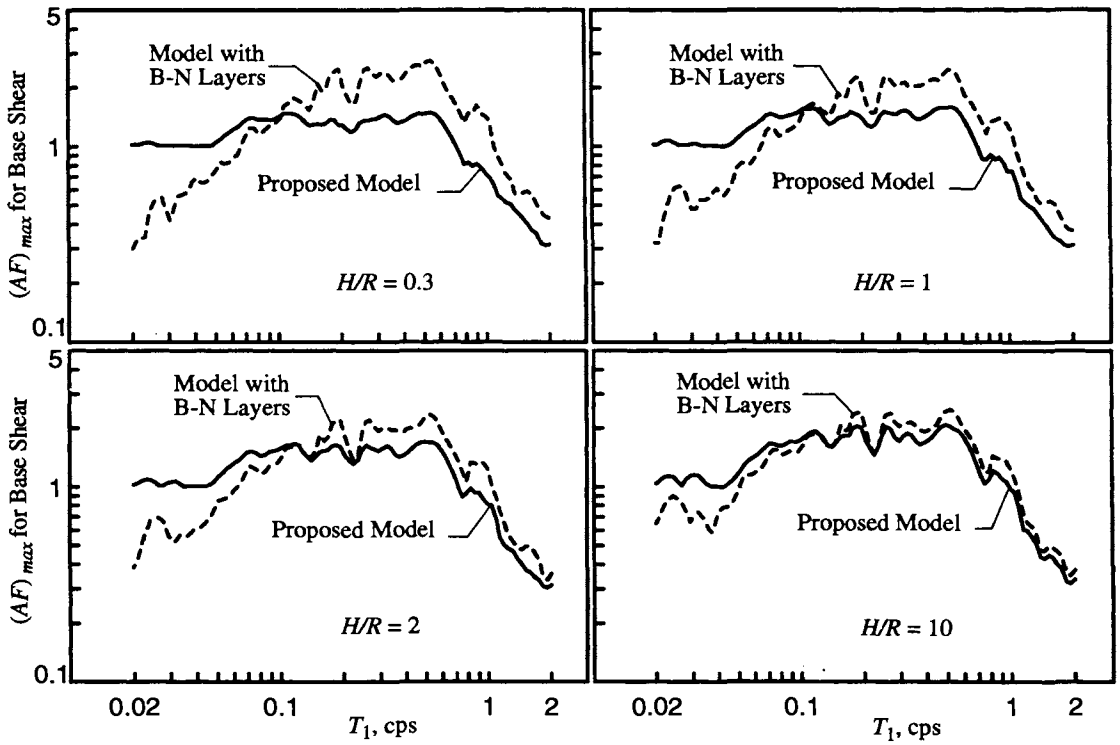

Fig. 22 Maximum amplification factor for amplitude of base shear induced by El Centro record; $\nu = 0.3$, $\delta = 0.1$

izontal shearing action and reduce the resulting wall forces. Additionally, the wall flexibility will increase the differences between the solutions obtained with the conventional, unconstrained layers and the proposed, constrained layers. By contrast, the presence of a flexible rather than rigid supporting medium will have the opposite effects. These effects will be addressed in future publications.

ACKNOWLEDGMENTS

These studies were carried out at Rice University under Project 568821 from Brookhaven National Laboratory, Upton, New York. This support is acknowledged gratefully. Appreciation also is expressed to Drs. M. Reich and K. Bandyopadhyay for helpful comments and their understanding project management.

REFERENCES

Alampalli, S., and Elgamal, A. W. (1991). "Retaining wall; computation of seismically induced deformations." *Proc. 2nd Int. Conf. on Recent Adv. in Geotech. Earthquake Eng. and Soil Dyn.*, St. Louis, Mo., University of Missouri, Rolla, Mo., Vol. I, pp. 635-642.

Arias, A., Sanchez-Sesma, F. J., and Ovando-Shelly, E. (1981). "A simplified elastic model for seismic analysis of earth-retaining structures with limited displacements." *Proc. Int. Conf. on Recent Adv. in Geotech. Earthquake Eng. and Soil Dyn.*, University of Missouri, Rolla, Mo., Vol. I, pp. 235-240.

Baranov V.A. (1967). "On the calculation of an embedded foundation," (Russian), *Voprosy Dinamiki i Prochnosti*, 14, Polytechnical Institute of Riga, Latvia, 195-209.

Beredugo, Y. O., and Novak, M. (1972). "Coupled horizontal and rocking vibration of embedded footings." *Canadian Geotech. J.*, 9 (4), 477-497.

Dennehy, K. T. (1984). "Seismic vulnerability, analysis and design of anchored bulkheads." Ph.D. thesis, Rensselaer Polytechnic Institute, Troy, N.Y.

Electrical Power Research Institute (1989), in *Proc. EPRI/ NRC/TPC Workshop on Seismic Soil-Structure Interaction Analysis Techniques Using Data from Lotung, Taiwan*, Vols. I and II, *Report NP-6154*, Palo Alto, CA.

Flores-Berrones, R., and Whitman, R. V. (1982). "Seismic response of end-bearing piles." *J. Geotech. Eng. Div. ASCE*, 108(4), 554-569.

Hadjian, A. H. et al (1991). "A synthesis of predictions and correlation studies of the Lotung soil-structure interaction experiment." *Report NP-7307-SL*, Electrical Power Research Institute, Palo Alto, CA.

Jain, S. K., and Scott, R. F. (1989). "Seismic analysis of cantilever retaining walls." *Proc. of Structural Mechanics in Reactor Technology*, Anaheim, Calif., pp. 241-246.

Karkanias, S. (1983). "Seismic behavior and simplified analysis of anchored sheet pile bulkheads." M.S. thesis, Rensselaer Polytechnic Institute, Troy, N.Y..

Miller, C. A., Costantino, C. J., and Heymsfeld, E. (1991). "Soil-structure interaction effects on high level waste tanks." *Proc. Third D.O.E. Natural Phenomena Hazards Mitigation Conf.*, St. Louis, Mo., Lawerence Livermore National Laboratory, Livermore, Calif., pp. 588-595.

Mononobe, N., and Matuo, H. (1929). "On the determination of earth pressures during earthquakes." *Proc. World Eng. Congress*, Tokyo, Japan, Vol. 9, Paper No. 388.

Nazarian, H. N., and Hadjian, A. H. (1979). "Earthquake-induced lateral soil pressures on structures." *J. Geotech. Eng. Div., ASCE,* 105(9), 1049-1066.

Nogami, T., and Novak, M. (1977). "Resistance of soil to a horizontally vibrating pile." *Earthquake Eng. & Struct. Dyn.*, 5 (3), 249-261.

Novak, M., and Beredugo, Y. O. (1972). "Vertical vibration of embedded footings," *J. Soil Mech. and Found. Div., ASCE,* 98 (12), 1291-1310.

Novak, M. (1974). "Dynamic stiffness and damping of piles." *Canadian Geotech. J.*, 11 (4), 574-598.

Okabe, S. (1924). "General theory of earth pressure and seismic stability of retaining wall and dam." *J. Japan Soc. Civil Engrs.*, Vol. 12.

Pais, A., and Kausel, E. (1988). "Approximate formulas for dynamic stiffnesses of rigid foundations." *Soil Dyn. & Earthquake Eng.*, 7 (4), 213-227.

Prakash, S. (1981). "Analysis of rigid retaining walls during earthquakes." *Proc. Int. Conf. on Recent Adv. in Geotech. Earthquake Eng. and Soil Dyn.*, University of Missouri, Rolla, Mo., Vol. III, pp. 1-28.

Roesset, J. M., Whitman, R. V., and Dobry, R. (1973). "Modal analysis for structures with foundation interaction." *J. Struct. Div., ASCE*, 99 (3), 399-416.

Scott, R. F. (1973). "Earthquake-induced pressures on retaining walls." *Proc. 5th World Conf. on Earthquake Eng.*, Rome, Italy, IAEE, Tokyo, Japan, Vol. II, 1611-1620.

Seed, H. B., and Whitman, R. V. (1970). "Design of earth retaining structures for dynamic loads." *ASCE Speciality Conf. on Lateral Stresses in the Ground and Design of Earth Retaining Structures*, pp. 103-147.

Sherif, M. A., Ishibashi, I. and Lee, C. D. (1982). "Earth pressure against rigid retaining walls." J. Geotech. Eng. Div. ASCE, 108(5), 679-695.

Sherif, M. A., and Fang, Y. F. (1984). "Dynamic earth pressures on walls rotating abouts the top." Soils and Foundations, 24, 109-117.

Siller, T. J., Christiano, P. P., and Bielak, J. (1991). "Seismic response of tied-back retaining walls." *Earthquake Eng. & Struct. Dyn.*, 20, 605-620.

Soydemir, C. (1991). "Seismic design of rigid underground walls in New England." *Proc. 2nd Int. Conf. on Recent Adv. in Geotech. Earthquake Eng. and Soil Dyn.*, University of Missouri, Rolla, Mo., Vol. I, pp. 613-620.

Tajimi, H. (1969). "Dynamic analysis of a structure embedded in an elastic stratum," *Proc. of 4th World Conf. on Earthquake Eng.*, San Diego, Chile, IAEE, Tokyo, Japan, III(A-6), 53-69.

Veletsos, A. S., and Dotson, K. W. (1988). "Horizontal impedances for radially inhomogeneous viscoelastic soil layers," *Earthquake Eng. & Struct. Dyn.*, 16 (7), 947-966.

Veletsos, A. S., and Tang, Y. (1990). "Deterministic assessment of effects of ground-motion incoherence." *J. Eng. Mech. Div., ASCE*, 116 (5), 1109-1124.

Veletsos, A. S., and Verbic, B. (1973). "Vibration of viscoelastic foundations." *Earthquake Eng. & Struct. Dyn.*, 2 (1), 87-102.

Veletsos, A. S., and Younan, A. H. (1994a). "Dynamic soil pressures on rigid vertical walls." *Earthquake Eng. & Struct. Dyn.*, 23 (3), 275-301.

Veletsos, A. S., and Younan, A. H. (1994b). "Dynamic soil pressures on rigid cylindrical vaults." *Earthquake Eng. & Struct. Dyn.*, 23 (6), 645-669.

Veletsos, A. S. and Younan A. H. (1994c). "Dynamic modeling and response of soil-wall systems," *J. Geotech. Eng. ASCE,* 120(12), 2155-2179.

Veletsos, A. S. and Younan, A. H. (1995). "Dynamic modeling and response of rigid embedded cylinders," to appear in September issue of *J. Eng. Mech. ASCE,* Paper 9394.

Whitman, R. V. (1991). "Seismic design of earth retaining structures." *Proc. 2nd Int. Conf. on Recent Adv. in Geotech. Earthquake Eng. and Soil Dyn.*, St. Louis, Mo., University of Missouri, Rolla, Mo., Vol. II, pp. 1767-1778.

Wood, J. H. (1973). "Earthquake-induced soil pressures on structures." *Report EERL 73-05*, Earthquake Engineering Research Laboratory, California Institute of Technology.

Wolf, J. P. (1988). *Soil-structure interaction analysis in time domain.* Prentice-Hall, Englewoods Cliffs, N. J., pp. 88-95.